

Terahertz radiation from a laser plasma filament

H.-C. Wu (武慧春),^{1,*} J. Meyer-ter-Vehn,¹ H. Ruhl,² and Z.-M. Sheng (盛政明)^{3,4}

¹Max-Planck-Institut für Quantenoptik, D-85748 Garching, Germany

²Department für Physik der Ludwig-Maximilians-Universität, Theresienstrasse 37A, D-80333 München, Germany

³Institute of Plasma Studies, Department of Physics, Shanghai Jiaotong University, Shanghai 200240, China

⁴Beijing National Laboratory of Condensed Matter Physics, Institute of Physics, CAS, Beijing 100190, China

(Received 13 May 2010; revised manuscript received 16 January 2011; published 15 March 2011)

By the use of two-dimensional particle-in-cell simulations, we clarify the terahertz (THz) radiation mechanism from a plasma filament formed by an intense femtosecond laser pulse. The nonuniform plasma density of the filament leads to a net radiating current for THz radiation. This current is mainly located within the pulse and the first cycle of the wakefield. As the laser pulse propagates, a single-cycle and radially polarized THz pulse is constructively built up forward. The single-cycle shape is mainly due to radiation damping effect.

DOI: [10.1103/PhysRevE.83.036407](https://doi.org/10.1103/PhysRevE.83.036407)

PACS number(s): 52.59.Ye, 42.65.Re, 52.25.Os, 52.38.Hb

I. INTRODUCTION

Since 1993, the pioneering experiments by Hamster *et al.* [1,2] observed strong terahertz (THz) wave generations when intense laser pulses are focused in gas or on solid targets. For the first time, these experiments demonstrated laser wakefield generation in the underdense plasma [3]. For the solid target, laser prepulse can generate a long underdense plasma on the target surface. THz emission from such a nonuniform plasma can be explained by linear mode conversion mechanism [4,5]. When the laser pulse is focused into the gas, due to the balance among natural diffraction, plasma defocusing, and Kerr self-focusing, a laser pulse carries out periodic defocusing and self-focusing, and can propagate a very long distance. After the laser pulse, a narrow and long plasma column, i.e., a laser filament, is formed.

Due to scientific motivations in unexplored THz electromagnetic spectrum and broad application prospects [6,7], developments on novel THz sources [8,9] have attracted great interest. As a simple and remote-distance THz source, THz radiation from the laser filament gains elaborate investigations [10–17]. Tzortzakis *et al.* [11] observed the THz radiation in the direction perpendicular to the filament. Theory and simulation investigations by Sprangle *et al.* [17] present an explanation for this radial-direction THz radiation. They found that, in the longitudinally density-modulated (due to periodic self-focusing and defocusing) filament, the plasma current or laser ponderomotive force has the superluminal Fourier components, which can emit a THz wave analogous to Cherenkov radiation. Most recently, experiments in Refs. [12,13] observed stronger radially polarized THz emissions along the laser propagation direction. They consider a light-speed dipolelike current in a limited-length plasma filament and calculate THz radiation using the theory developed in Ref. [18]. The radiation current is simply assumed to be a laser-driven longitudinal plasma wave, which decays due to plasma collisions.

In the present work, by analysis and two-dimensional (2D) particle-in-cell (PIC) simulation, we find that crossing coupling between electron current and density gradient [19,20]

is responsible for these forward THz radiations. At first, the laser ponderomotive force pushes the electrons and induces space charge fields. The electron current oscillates forward and backward in the electrostatic wakefield. When the electrons pass by the transverse boundary of the filament, the coupling between electron motion and nonuniform density gradient induces a net radiating current, which is a small part of the total electron current. The radiating current is mainly located within the laser pulse and the first cycle of the wakefield. It is just like a dipole propagating with the laser pulse and builds up a monocycle THz pulse in the forward direction. THz radiation is radially polarized and should show a double-lobe pattern in the far field. We also point out that radiation reaction damps the THz pulse into single-cycle profile.

II. THZ GENERATION FROM A PLASMA FILAMENT

We consider a short filament in the tenuous gas as Refs. [12,13], where the laser pulse is tightly focused and the filament length is limited and on the order of laser Rayleigh length. In Ref. [17], THz radiation from a long filament is analyzed and simulated. For a steady-state laser filament, there is no electromagnetic radiation and only a surface electromagnetic wave [21] is generated. The steady state means that both the laser pulse and plasma density are independent of the propagation distance. This is not the case for an actual filament, because the laser filament is a highly nonlinear and dynamical process [22]. We also consider a high laser intensity of above 10^{15} W/cm², and tunneling ionization is dominant for plasma formation. During the short rising time of the pulse, atoms are ionized, and then the main pulse interacts with the plasma. In our case, the laser filament is mainly determined by the initial focusing and plasma defocusing. Kerr effect can be negligible and pulse split does not occur.

From the 2D PIC simulation [23,24], a short filament after the laser pulse is shown in Fig. 1(a). The laser pulse (*s*-polarized) propagates from left to right and its geometric focus is at $x = 100\lambda_0$ ($\lambda_0 = 800$ nm). The pulse has the shape $\sin^2(\pi t/T)$ with $T = 20\tau_0$ and the Gaussian waist size $W = 2.5\lambda_0$. The peak intensity is about $I = 5.35 \times 10^{15}$ W/cm². We choose He gas with density $0.0025n_c$ within $x \in [5\lambda_0, 195\lambda_0]$; n_c is the critical plasma density for the laser.

*Present address: Los Alamos National Laboratory, Los Alamos, New Mexico 87545, USA. E-mail: hcwu@lanl.gov

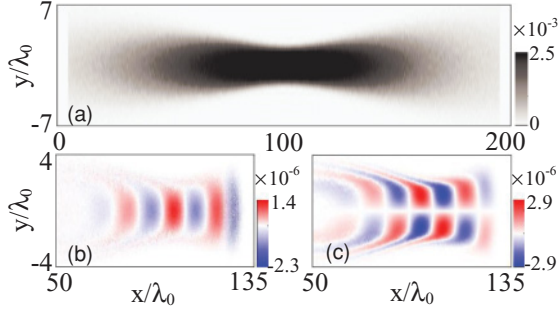


FIG. 1. (Color online) (a) Plasma density (unit n_c) of the filament after the laser pulse; (b) longitudinal electron current J_x (unit $en_c c$) and (c) transverse current J_y at $t = 140\tau_0$.

Around the laser focus, all He atoms are ionized and each one loses one electron. So, the peak plasma density in the filament is $n_{e0} = 0.0025n_c$, which corresponds to a plasma wavelength $\lambda_p = 20\lambda_0$. The plasma density is maximum on the center of the filament. The filament length with the density above $0.5n_{e0}$ is about $120\lambda_0$. The density linearly increases from $0.16n_{e0}$ to n_{e0} within $x \in [5\lambda_0, 70\lambda_0]$. The slowly varying plasma density ensures that the electromagnetic radiations come from the filament body, instead of plasma surfaces. The filament diameter at light focus is about $4\lambda_0$.

The laser pulse pushes the electrons by the ponderomotive force and induces both longitudinal current J_x [Fig. 1(b)] and transverse current J_y [Fig. 1(c)]. The currents oscillates with the plasma frequency $\omega_{p0} = \sqrt{e^2 n_{e0} / \epsilon_0 m} = 0.05\omega_0$. These currents may generate the p -polarized electromagnetic wave radiation. The magnetic component B_z is plotted in Fig. 2(a). A single-cycle THz pulse is emitted from the plasma filament and copropagates with the laser pulse. In the 3D space, the THz radiation should be radially polarized in the far field and null along the laser axis. In the far field, its energy-flux pattern should be double lobe. This agrees with the experiments [12,13]. The THz pulse shape traced at $[x, y] = [200\lambda_0, -60\lambda_0]$ and the corresponding spectrum are illustrated in Figs. 2(b) and 2(c). The THz frequency is broad and around the plasma frequency ω_{p0} . The longer laser pulse leads to the lower central frequency.

We input the plasma density in Fig. 1(a) into a conventional PIC simulation without the ionization process, and find that

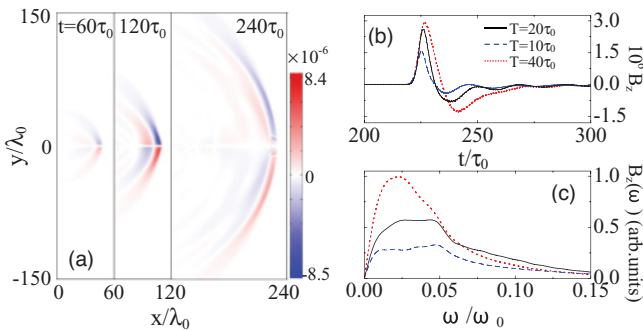


FIG. 2. (Color online) (a) Radiating magnetic field B_z at $t = 60\tau_0$, $120\tau_0$, and $240\tau_0$; the temporal shape (b) and the spectrum (c) of B_z pulses traced at $[x, y] = [200\lambda_0, -60\lambda_0]$. (b) and (c) also include the results for the laser durations $T = 10\tau_0$ and $40\tau_0$.

main characteristics remain the same. These are slightly different from the THz spatial distribution in Fig. 2(a), due to the preformed plasma column instead of instantaneous plasma formation. In an approximate way, the problem can be reduced to the interaction between the laser and one plasma column. In passing, the laser pulse in our case is long and the ionization-induced THz radiation (s -polarized as the laser) [24,25] is negligible.

In the following, we will clarify the reason why there is the THz radiation from the filament. For a general electromagnetic system, the electromagnetic radiation equation (Coulomb gauge) is

$$\left(\nabla^2 - \frac{1}{c^2} \frac{\partial^2}{\partial t^2}\right) \mathbf{A}_r = -\mu_0 \mathbf{J}_r, \quad (1)$$

where $\mathbf{J}_r = \mathbf{J} - \frac{1}{c^2} \frac{\partial}{\partial t} \nabla \phi_w$ is the radiating current [26], i.e., the rotational part of the total current \mathbf{J} , and ϕ_w is the electrostatic potential of the wakefield, which satisfies $\nabla^2 \phi_w = e(Zn_i - n_e)/\epsilon_0$. The total electric field is $\mathbf{E} = \mathbf{E}_r + \mathbf{E}_w$; here the radiating field $\mathbf{E}_r = -\frac{\partial}{\partial t} \mathbf{A}_r$ and the wakefield $\mathbf{E}_w = -\nabla \phi_w$. The existent electromagnetic radiation implies the nonzero \mathbf{J}_r , which demands $\nabla \times \mathbf{J} \neq 0$.

For our case, the dimensionless amplitude of the laser pulse $a = eE_L/mc\omega_0 = 0.05$. We can use the linear plasma theory [20,27], which is valid for $a^2 \ll 1$. On the order of $O(a)$, the electron carries out the oscillation with the light frequency. On the order of $O(a^2)$, the electron motion equation is

$$\frac{\partial}{\partial t} \mathbf{v} = \frac{-e}{m} (\mathbf{E}_r + \mathbf{E}_w) + \frac{1}{m} \mathbf{F}_p, \quad (2)$$

where $\mathbf{F}_p = -mc^2 \nabla(a^2/2)$ is the 3D ponderomotive force of the laser pulse in the linear limit [3]. Combining Eq. (2) and $\nabla \times \mathbf{E}_r = -\partial \mathbf{B}_r / \partial t$ gets

$$\nabla \times \mathbf{v} = \frac{e}{m} \mathbf{B}_r, \quad (3)$$

which displays that the curl of the velocity of the electron fluid is the magnetic component of the radiation field. For the radiation field in vacuum and far away from the laser pulse, Eq. (2) becomes $\frac{\partial}{\partial t} \mathbf{v} = \frac{-e}{m} \mathbf{E}_r$, where \mathbf{v} is only an intermediary quantity between \mathbf{E}_r and \mathbf{B}_r . Making the time derivative of Eq. (2), and using $\nabla \times \mathbf{B}_r = \mu_0 \mathbf{J} + \mu_0 \epsilon_0 \partial \mathbf{E} / \partial t$ and Eq. (3), one obtains

$$\frac{\partial^2}{\partial t^2} \mathbf{v} + c^2 \nabla \times \nabla \times \mathbf{v} + \omega_p^2 \mathbf{v} = \frac{1}{m} \frac{\partial}{\partial t} \mathbf{F}_p. \quad (4)$$

Once the electron velocity \mathbf{v} is solved from Eq. (4), the radiation field can be obtained by Eq. (3). The curl of the total current reads

$$\nabla \times \mathbf{J} = -e \nabla n_e \times \mathbf{v} - en_e \nabla \times \mathbf{v}. \quad (5)$$

In the infinitely uniform plasma ($\omega_p^2 = \text{const.}$ or $\nabla n_e = 0$), Eq. (4) implies $\nabla \times \mathbf{v} = 0$ and then one has $\nabla \times \mathbf{J} = 0$. So, for the uniform plasma, there is no electromagnetic radiation on the order of $O(a^2)$. There is nonzero $\nabla \times \mathbf{v}$ on the order $O(a^4)$ for quasisteady magnetic field [20] and $2\omega_p$ radiation field [28] generations, which are important when the laser intensity approaches the relativistic intensity ($a \sim 1$), and is negligible for our case.

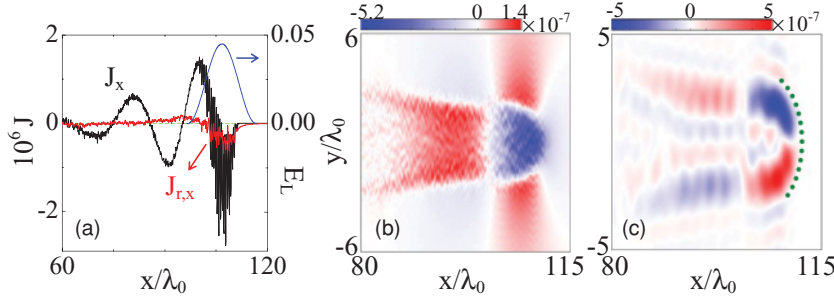


FIG. 3. (Color online) (a) Laser envelope, electron current J_x , and its rotational component $J_{r,x}$ at $t = 120\tau_0$ on the light axis; 2D plot of $J_{r,x}$ (b) and $\nabla \times J$ (c) at $t = 120\tau_0$; the dotted line in (c) represents the ionization front.

In fact, the observed THz radiation in the near field region in Fig. 2 is comparable with the wakefield, which is on the order of $O(a^2)$. The filament is a narrow plasma column and has a sharp transverse boundary and ionization front, because the tunneling ionization rate is exponentially dependent on the light field strength. Apparently, $e\nabla n_e \times \mathbf{v}$ is nonzero in Eq. (5) and responsible for THz generation in the filament. Making the curl of Eq. (1) and using Eqs. (3) and (5), one has

$$\left(\nabla^2 - \frac{1}{c^2} \frac{\partial^2}{\partial t^2} + \frac{\omega_p^2}{c^2} \right) \mathbf{B}_r = \mu_0 e \nabla n_e \times \mathbf{v}, \quad (6)$$

which is the radiation wave equation for \mathbf{B}_r . In the 2D case, the source term $\nabla n_e \times \mathbf{v} = (v_y \partial n_e / \partial x - v_x \partial n_e / \partial y) \hat{z}$, the cross coupling between the electron velocity and density gradient, is responsible for THz magnetic field B_z in Fig. 2. The quasistatic magnetic field generation from a nonuniform plasma has been discussed in Ref. [19]. An approximate solution \mathbf{v} in Eq. (4) can be obtained by first assuming $\nabla \times \mathbf{v} = 0$. Then the solution is well known as

$$\mathbf{v} = (m\omega_p)^{-1} \int_{-\infty}^t dt' \sin \omega_p(t-t') \partial \mathbf{F}_p(t') / \partial t', \quad (7)$$

by which the currents in Fig. 1 can be analytically reproduced well. Substituting \mathbf{v} into Eq. (6), an analytic solution can be obtained as done in Ref. [28]. However, this approach is not consistent, because it does not take into account the self-action of the radiation field and cannot give the correct temporal shape of the THz wave.

Numerically, we can extract the rotational part from the total current \mathbf{J} , i.e., radiating current \mathbf{J}_r . Figures 3(a) and 3(b) show that the radiating current $J_{r,x}$ is one fraction of the total current J_x . $J_{r,x}$ is single cycle as the THz pulse. Figure 3(c) shows the curl of \mathbf{J} , which is mainly located in the transverse border of the filament. The plasma density is relatively uniform around the filament axis, where $\nabla \times \mathbf{J} \approx 0$. In 3D space, $\nabla \times \mathbf{J}$ is similar to a magnetic dipole pointing to the laser direction. We find that J_x has dominant contributions to \mathbf{J}_r and $\nabla \times \mathbf{J}$, compared with J_y . So, in general, we can say that the cross coupling between v_x and $\partial n_e / \partial y$ is the main mechanism for THz radiation. Electrons longitudinally sweep the transverse nonuniform plasma in the filament boundary and excite the THz radiation.

One interesting thing is that the current is multicycle, however, the radiating current is monocycle. This is due to the self-action of the radiation field. It is shown that the solution of Eq. (6) [28] is damping with time. The damping effect is due to the term $\frac{\omega_p^2}{c^2} \mathbf{B}_r$, which is the radiation reaction effect. The origin is from the term $\frac{-e}{m} \mathbf{E}_r$ in the electron motion Eq. (2). As soon

as the radiation appears, \mathbf{v} will have a rotational component \mathbf{v}_r , which satisfies the rotational component of Eq. (2),

$$\frac{\partial}{\partial t} \mathbf{v}_r = \frac{-e}{m} \mathbf{E}_r. \quad (8)$$

The radiation field \mathbf{E}_r of a radiating current directly damps itself by Eq. (8). Since there is only one-time impulse from the single laser pulse, this radiation damping effect is very strong and leads to a single-cycle radiation. If a multiple pulse train with proper separation is used, THz radiation can be multicycle. A consistent investigation on the radiation damping effect needs the numerical solution of Eq. (4). The radiation damping also has the same effects on the ionization-induced THz radiation produced by an isolated few-cycle laser pulse [24,25,29,30] or two-color laser waves [31–34].

III. DISCUSSIONS AND CONCLUSIONS

The THz radiation mechanism discussed here also provides a simpler and more intuitive explanation for Ref. [23], where a powerful single-cycle THz pulse is generated when a intense laser pulse is obliquely incident on a plasma slab with sharp boundaries. A 1D analytic scaling obtained in the boosted frame predicts THz amplitude $E_T \propto n_{e0}^{1/2} a^2 \sin \theta$ [23], where θ is the incident angle. Since there is the source term $\nabla n_e \times \mathbf{v}$ in Eq. (6), $\mathbf{v} \propto n_{e0}^{-1/2} a^2$ from Eq. (7), and $\nabla n_e = n_{e0} \delta(x)$ around a sharp boundary, one can easily gets $\nabla n_e \times \mathbf{v} \propto n_{e0}^{1/2} a^2 \sin \theta$, where θ is the separate angle between the density gradient ∇n_e and electron velocity \mathbf{v} (i.e., laser direction). For the normal incidence ($\theta = 0$) of Gaussian laser beams on the vacuum-plasma boundary, THz radiation by the term $\nabla n_e \times \mathbf{v}$ had been discussed in Ref. [35].

In conclusion, we clarify THz radiation mechanism from a laser plasma filament. The laser pulse pushes the electrons along the laser direction. The cross coupling between longitudinal electron motion and transverse density gradient leads to forward THz radiation. Radiation damping effect shapes THz wave into a monocycle profile.

ACKNOWLEDGMENTS

H.-C. Wu acknowledges support from the Alexander von Humboldt Foundation. Z.-M. Sheng was supported by the National Basic Research Program of China under Grants No. 2007CB310406 and No. 2009GB105002.

- [1] H. Hamster, A. Sullivan, S. Gordon, W. White, and R. W. Falcone, *Phys. Rev. Lett.* **71**, 2725 (1993).
- [2] H. Hamster, A. Sullivan, S. Gordon, and R. W. Falcone, *Phys. Rev. E* **49**, 671 (1994).
- [3] E. Esarey, P. Sprangle, J. Krall, and A. Ting, *IEEE Trans. Plasma Sci.* **24**, 252 (1996).
- [4] Z.-M. Sheng, K. Mima, J. Zhang, and H. Sanuki, *Phys. Rev. Lett.* **94**, 095003 (2005).
- [5] Z.-M. Sheng, K. Mima, and J. Zhang, *Phys. Plasmas* **12**, 123103 (2005).
- [6] B. Ferguson and X.-C. Zhang, *Nat. Mater.* **1**, 26 (2002).
- [7] *Opportunities in THz Science*, Report of a DOE-NSF-NIH Workshop held February 12–14, 2004, Arlington, VA, edited by M. S. Sherwin, C. A. Schmuttenmaer, and P. H. Bucksbaum.
- [8] G. P. Williams, *Rep. Prog. Phys.* **69**, 301 (2006).
- [9] K. Reimann, *Rep. Prog. Phys.* **70**, 1597 (2007).
- [10] A. Couairon and A. Mysyrowicz, *Phys. Rep.* **441**, 47 (2007).
- [11] S. Tzortzakis, G. Mechkain, G. Patalano, Y.-B. Andre, B. Prade, M. Franco, A. Mysyrowicz, J.-M. Munier, M. Gheudin, G. Beaudin, and P. Encrenaz, *Opt. Lett.* **27**, 1944 (2002).
- [12] C. D'Amico, A. Houard, M. Franco, B. Prade, A. Mysyrowicz, A. Couairon, and V. T. Tikhonchuk, *Phys. Rev. Lett.* **98**, 235002 (2007).
- [13] C. D. Amico, A. Houard, S. Akturk, Y. Liu, J. Le Bloas, M. Franco, B. Prade, A. Couairon, V. T. Tikhonchuk, and A. Mysyrowicz, *New J. Phys.* **10**, 013015 (2008).
- [14] Y. Liu, A. Houard, B. Prade, S. Akturk, A. Mysyrowicz, and V. T. Tikhonchuk, *Phys. Rev. Lett.* **99**, 135002 (2007).
- [15] A. Houard, Y. Liu, B. Prade, V. T. Tikhonchuk, and A. Mysyrowicz, *Phys. Rev. Lett.* **100**, 255006 (2008).
- [16] Y. Liu, A. Houard, B. Prade, A. Mysyrowicz, A. Diaw, and V. T. Tikhonchuk, *Appl. Phys. Lett.* **93**, 051108 (2008).
- [17] P. Sprangle, J. R. Penano, B. Hafizi, and C. A. Kapetanakis, *Phys. Rev. E* **69**, 066415 (2004).
- [18] J. Zheng, C. X. Yu, Z. J. Zheng, and K. A. Tanaka, *Phys. Plasmas* **12**, 093105 (2005).
- [19] V. K. Tripathi and C. S. Liu, *Phys. Plasmas* **1**, 990 (1994).
- [20] L. M. Gorbunov, P. Mora, and T. M. Antonsen Jr., *Phys. Plasmas* **4**, 4358 (1997).
- [21] L. M. Gorbunov, P. N. Lebedev, P. Mora, and R. R. Ramazashvili, *Phys. Plasmas* **10**, 4563 (2003).
- [22] L. Berg, S. Skupin, R. Nuter, J. Kasparian, and J. P. Wolf, *Rep. Prog. Phys.* **70**, 1633 (2007).
- [23] H.-C. Wu, Z.-M. Sheng, and J. Zhang, *Phys. Rev. E* **77**, 046405 (2008).
- [24] H.-C. Wu, J. Meyer-ter-Vehn, and Z.-M. Sheng, *New J. Phys.* **10**, 043001 (2008).
- [25] V. B. Gildenburg and N. V. Vvedenskii, *Phys. Rev. Lett.* **98**, 245002 (2007).
- [26] J. D. Jackson, *Classical Electrodynamics* (Wiley, New York, 1998), p. 241.
- [27] N. E. Andreeva, L. M. Gorbunov, V. I. Kirsanov, K. Nakajima, and A. Ogata, *Phys. Plasmas* **4**, 1145 (1997).
- [28] Z.-M. Sheng, J. Meyer-ter-Vehn, and A. Pukhov, *Phys. Plasmas* **5**, 3764 (1998).
- [29] M. Kieß, T. Löffler, M. D. Thomson, R. Dörner, H. Gimpel, K. Zrost, T. Ergler, R. Moshhammer, U. Morgner, J. Ullrich, and H. G. Roskos, *Nature Phys.* **2**, 327 (2006).
- [30] A. M. Bystrov and V. B. Gildenburg, *Phys. Rev. Lett.* **103**, 083401 (2009).
- [31] X. Xie, J. Dai, and X.-C. Zhang, *Phys. Rev. Lett.* **96**, 075005 (2006).
- [32] K. Y. Kim, J. H. Glowina, A. J. Taylor, and G. Rodriguez, *Opt. Express* **15**, 4577 (2007).
- [33] K. Y. Kim, A. J. Taylor, J. H. Glowina, and G. Rodriguez, *Nat. Photon.* **2**, 605 (2008).
- [34] J.-M. Manceau, A. Averchi, F. Bonaretti, D. Faccio, P. Di Trapani, A. Couairon, and S. Tzortzakis, *Opt. Lett.* **34**, 2165 (2009).
- [35] L. M. Gorbunov and A. A. Frolov, *Plasma Phys. Rep.* **32**, 850 (2006).